The ionosphere under extremely prolonged low solar activity

Libo Liu,[1,2] Yiding Chen,[1] Huijun Le,[1] Vladimir I. Kurkin,[3] Nelya M. Polekh,[3] and Chien-Chih Lee[4]

Received 19 November 2010; revised 7 February 2011; accepted 11 February 2011; published 27 April 2011.

[1] A critical question in ionospheric physics is the state of the ionosphere and relevant processes under extreme solar activities. The solar activity during 2007–2009 is extremely prolonged low, which offers us a unique opportunity to explore this issue. In this study, we collected the global ionosonde measurements of the F_2 layer critical frequency (f_oF_2), E layer critical frequency (f_oE), and F layer virtual height ($h'F$) and the total electron content (TEC) maps produced by the Jet Propulsion Laboratory, which were retrieved from dual-frequency GPS receivers distributed worldwide, to investigate the ionospheric phenomena during solar minimum of cycle 23/24, particularly the difference in the ionosphere between solar minima of cycle 23/24 and the preceding cycles. The analysis indicates that the moving 1 year mean f_oF_2 at most ionosonde stations and the global average TEC went to the lowest during cycle 23/24 minimum. The solar cycle differences in f_oF_2 minima display local time dependence, being more negative during the daytime than at night. Furthermore, the cycle difference in daytime f_oF_2 minima is about −0.5 MHz and even reaches to around −1.2 MHz. In contrast, a complex picture presents in global $h'F$ and f_oE. Evident reduction exists prevailingly in the moving 1 year mean $h'F$ at most stations, while no huge differences are detected at several stations. A compelling feature is the increase in f_oE at some stations, which requires independent data for further validation. Quantitative analysis indicates that record low f_oF_2 and low TEC can be explained principally in terms of the decline in solar extreme ultraviolet irradiance recorded by SOHO/SEM, which suggests low solar EUV being the prevailing contributor to the unusual low electron density in the ionosphere during cycle 23/24 minimum. It also verifies that a quadratic fitting still reasonably captures the solar variability of f_oF_2 and global average TEC at such low solar activity levels.

Citation: Liu, L., Y. Chen, H. Le, V. I. Kurkin, N. M. Polekh, and C.-C. Lee (2011), The ionosphere under extremely prolonged low solar activity, *J. Geophys. Res.*, *116*, A04320, doi:10.1029/2010JA016296.

1. Introduction

[2] The solar activity in 2007–2009 was extremely prolonged low, which created a record for spotless days over recent several solar cycles. The end of the solar minimum of solar cycle 23 came later at least 2 years than was expected. As a result, the solar minimum of solar cycle 23/24 was abnormal and quite different from the preceding solar cycles; many interesting phenomena occurred in the geospace [*Emmert et al.*, 2010; *Gibson et al.*, 2009; *Heelis et al.*, 2009; *Solomon et al.*, 2010].

[3] The solar activity is the primary controller for the structure and evolution of the geospace, particularly for the upper atmosphere and ionosphere [*Gorney*, 1990; *Liu et al.*, 2011]. Although most interest of the community is given to high solar activities, especially severe storm events, the study of the ionosphere under low solar activity conditions is also very essential. The significance of understanding the solar minimum lies in revealing the nature of solar variability, assessing the predictability of current models, and understanding the drivers of global climate and upper atmosphere changes [*Laštovička et al.*, 2006], particularly separating the climatic effects of solar sources from those of anthropogenic sources [e.g., *Solomon et al.*, 2010]. Huge interest has been stimulated to investigate the solar activity abnormalities and their consequences on the Earth's environment [e.g., *Russell et al.*, 2010; *Smithtro and Sojka*, 2005]. *Smithtro and Sojka* [2005] described the climatological behaviors in the upper atmosphere at extremely low and high solar activity levels, on the basis of several designed simulation results using their 1-D global average ionosphere and thermosphere model. According to their

[1]Beijing National Observatory of Space Environment, Institute of Geology and Geophysics, Chinese Academy of Sciences, Beijing, China.
[2]Also at State Key Laboratory of Space Weather, Center for Space Science and Applied Research, Chinese Academy of Sciences, Beijing, China.
[3]Institute of Solar-Terrestrial Physics, Russian Academy of Sciences, Irkutsk, Russia.
[4]General Education Center, Ching-Yun University, Jhungli, Taiwan.

0148-0227/11/2010JA016296

model results, the concentration of O^+ ions decreases very quickly relative to the molecular ions, when the solar irradiance falls below the normal solar minimum levels. *Russell et al.* [2010] overviewed our current understanding of the solar activity and how unprecedented solar cycle 23 might be. Through analyzing the solar extreme ultraviolet (EUV) irradiance recorded by the Solar EUV Monitor (SEM) [*Judge et al.*, 1998] on the Solar and Heliospheric Observatory (SOHO), *Solomon et al.* [2010] found ~15% reduction in solar EUV irradiance in 2008, compared to that in 1996. *Chen et al.* [2011] revealed that SOHO/SEM EUV flux in the current solar minimum is remarkably different from that in the last one. Furthermore, in 2008–2009 the upper atmosphere became cooler and the thermospheric density anomalously went to record low [*Solomon et al.*, 2010; *Emmert et al.*, 2010], according to the analyses of the historical archive of satellite orbital elements from thousands of man-made orbit objects over many decades. In particular, the retrieved thermospheric density at 400 km was found to be unusually low by 30% in 2009 [*Emmert et al.*, 2010]. Model simulations showed fascinating evidence that the unusually low level of solar EUV was the primary cause of the low thermospheric density in 2007–2009, while increasing anthropogenic CO_2 can only account for a much smaller part of the changes in thermospheric temperature and density [*Solomon et al.*, 2010].

[4] Unusual changes are also detected in the ionosphere during this period. By investigating the major ion compositions and other parameters measured by the Air Force Communications Navigation Outage Forecast System (C/NOFS) satellite, *Heelis et al.* [2009] described the behavior of the topside ionosphere during the solar minimum of 2008. The O^+/H^+ transition height, as an indicator of the height of the topside ionosphere [*Kutiev and Marinov*, 2007], is found to reside near 450 km at night and 850 km during the day, much lower than the predicted values of the International Reference Ionosphere (IRI) model [e.g., *Bilitza and Reinisch*, 2008]. Both the concentrations and temperature of the ions in the topside ionosphere were lower than the predicted values. *Heelis et al.* [2009] suggested that the ionosphere is contracted and the dynamics of the ionosphere is significantly different from our expectations. Furthermore, *Lühr and Xiong* [2010] compared the in situ measurements of the CHAMP and GRACE satellites in the years 2000–2009 with the IRI-2007 predictions. They found that the electron density values of IRI-2007 model track the measurements reasonably well during the period 2000–2004, but turn to overestimate the observations in the later period, being high by 50% for 2008 and more than 60% in 2009. The model's unexpected overestimation in 2008–2009 suggests that the ionosphere has also experienced fundamental modifications during the deep solar minimum [*Lühr and Xiong*, 2010].

[5] In this study, our intention is to demonstrate the unusual phenomena in the global ionosphere during the deep solar minimum in 2007–2009. We collected the F_2 layer critical frequency (f_oF_2), E layer critical frequency (f_oE), and F layer virtual height ($h'F$) data recorded at global ionosonde stations. We also took the total electron content (TEC) data, which were retrieved at Jet Propulsion Laboratory (JPL) from dual-frequency Global Positioning System (GPS) receivers distributed worldwide in the format of Global Ionospheric Maps (GIMs) [*Mannucci et al.*, 1998]. Based on the combination of the above data sets and the solar data, we conducted an analysis to characterize the unique nature of the ionosphere during the solar minima of cycle 23/24, particularly the difference in the ionosphere between the solar minima of cycle 23/24 and the preceding cycles. It is the first time to report that record low f_oF_2 and low TEC occurred globally during this solar minimum, accompanying with a decline in $h'F$. The most compelling feature is the increase in f_oE, but the behaviors of f_oE are not consistent globally. Another aim of this study is to test the ability of a quadratic fitting to statistically capture the solar variability of f_oF_2 and global average TEC at such low solar activity levels.

2. Data Source

2.1. Ionosonde f_oF_2, f_oE, and $h'F$

[6] Ionosonde data of f_oF_2 (in MHz), f_oE (in MHz), and $h'F$ (in km) recorded over the past several solar cycles were analyzed in this study. We collected the ionosonde data recorded globally at more than 170 stations, which are available from the SPIDR website (http://spidr.ngdc.noaa.gov/) and from National Institute of Information and Communications Technology of Japan and at Irkutsk (52.5°N, 104.0°E) station of Russia. A map for these stations can be found at the SPIDR website and also in Figure 1 of *Liu et al.* [2010].

[7] It is well known that the ionosphere varies with solar activity, season, and local time. To decrease possible influences of short-period fluctuations, e.g., the seasonal effect and day-to-day variability, a moving 1 year average has been applied to smooth f_oF_2 and other parameters at individual stations. When the amount of record points in a moving 1 year window is below a threshold, we did not evaluate the mean value for the window. The threshold we taken is 180 data points at a specified local time in a moving 1 year window. We discarded the station if the 1 year mean points there are not simultaneously available during the solar minima of cycle 23/24 and in the preceding cycles for comparison. At these stations, there should have data points to determine the lowest values around solar minimum in the past cycles. We take the minimum among the solar minimum values for comparing with the cycle 23/24. As a result, there are 31 stations finally available for f_oF_2, 20 stations for $h'F$, and 21 stations for f_oE. Table 1 lists the key information of the stations for our analysis. With the moving 1 year mean data, we can determine the differences of the parameters minima at solar minima between different solar cycles at specified local times.

2.2. JPL GPS TEC

[8] The data of total electron content (TEC) in the ionosphere for this analysis are collected from the global ionospheric maps (GIMs) provided at the Jet Propulsion Laboratory (JPL) website. The TEC GIMs can be derived from the worldwide observations of dual-frequency GPS receivers. The deriving procedure of JPL TEC has been described by *Mannucci et al.* [1998]. JPL and other analysis centers have routinely produced GIMs with a 2 h temporal resolution and a spatial resolution of 5° in longitude and 2.5° in latitude since 1998 [e.g., *Iijima et al.*, 1999;

Table 1. The Coordinates of Ionosonde Where f_oF_2, $h'F$, or f_oE Parameters Were Analyzed in the Study

URSI Code	Station Name	Apex Latitude (deg)	Geographic Latitude (deg)	Geographic Longitude (deg)	Parameters	Total Days
CW46O	Casey	−80.59	−66.3	110.6	f_oF_2, -, -	5291, -, -
MW26P	Mawson	−70.51	−67.6	62.9	f_oF_2, -, -	9252, -, -
MQ55M	Macquarie Is.	−64.13	−54.5	159.0	f_oF_2, -, -	5192, -, -
HO54K	Hobart	−53.74	−42.9	147.3	f_oF_2, f_oE, $h'F$	16713, 8632, 8201
CB53N	Canberra	−45.26	−35.3	149.1	f_oF_2, f_oE, $h'F$	16175, 9044, 7494
MU43K	Mundaring	−44.04	−32.0	116.4	f_oF_2, -, -	12604, -, -
CN53L	Camden	−43.65	−34.0	150.7	f_oF_2, -, -	6826, -, -
GR13L	Grahamstown	−41.35	−33.3	26.5	f_oF_2, f_oE, $h'F$	9185, 8420, 9401
PSJ5J	Port Stanley	−38.14	−51.7	302.2	f_oF_2, f_oE, $h'F$	13320, 6832, 11174
BR52P	Brisbane	−35.35	−27.5	152.9	f_oF_2, f_oE, $h'F$	13778, 5938, 5759
NI63_	Norfolk	−35.60	−29.0	168.0	f_oF_2, f_oE, $h'F$	11356, 6659, 5702
TV51R	Townsville	−28.64	−19.7	146.9	f_oF_2, f_oE, -	15351, 9269, -
DW41K	Darwin	−21.80	−12.5	131.0	f_oF_2, f_oE, -	5390, 3546, -
VA50L	Vanimo	−11.02	−2.7	141.3	f_oF_2, f_oE, $h'F$	10159, 6106, 6487
JI91J	Jicamarca	0.39	−12.1	283.0	f_oF_2, -, -	2749, -, -
OK426	Okinawa	19.17	26.3	127.8	f_oF_2, f_oE, $h'F$	9467, 4899, 6902
YG431	Yamagawa	24.13	31.2	130.6	f_oF_2, f_oE, $h'F$	10604, 6783, 8137
TO535	Kokubunji	28.45	35.7	139.5	f_oF_2, -, $h'F$	17760, -, 14736
EA036	El Arenosillo	31.01	37.1	353.3	f_oF_2, f_oE, -	2904, 2838, -
EB040	Del'ebre	35.10	40.8	0.3	f_oF_2, f_oE, $h'F$	11447, 10625,10497
RO041	Rome	36.04	41.8	12.5	f_oF_2, f_oE, -	14367, 8490, -
WK545	Wakkanai	38.40	45.4	141.7	f_oF_2, f_oE, $h'F$	16943, 10845,13363
PA836	Point Arguello	41.18	35.6	239.4	f_oF_2, f_oE, $h'F$	9396, 7233, 8093
PQ052	Pruhonice	45.49	50.0	14.6	f_oF_2, -, -	6346, -, -
DB049	Dourbes	46.00	50.1	4.6	f_oF_2, f_oE, $h'F$	10687, 8212, 10981
IR352	Irkutsk	47.17	52.5	104.0	f_oF_2, -, -	12518, -, -
RL052	Chilton	48.18	51.6	358.7	-, -, $h'F$	-, -, 4762
WP937	Wallops Is.	48.36	37.8	284.5	f_oF_2, f_oE, $h'F$	9103, 7258, 9381
BC840	Boulder	48.69	40.0	254.7	f_oF_2, f_oE, $h'F$	15348, 12491,14849
JR055	Juliusruh/R.	50.73	54.6	13.4	f_oF_2, f_oE, $h'F$	16159, 10210,16260
GSJ53	Goosebay	61.18	53.3	299.6	f_oF_2, f_oE, -	5653, 4766, -
TR169	Tromso	66.53	69.7	19.0	-, -, $h'F$	-, -, 2960
THJ77	Thule/Qanaq	85.14	77.5	290.8	f_oF_2, -, $h'F$	5238, -, 7550

Mannucci et al., 1998], which provides excellent database for ionospheric studies. We have analyzed these data particularly to diagnose the average behavior and solar activity dependence of GPS TEC [*Liu and Chen*, 2009; *Liu et al.*, 2009].

[9] The JPL GIMs data on every day from its open release in 1998 to October 2010 were globally averaged to calculate the daily global average TEC in the similar way of *Hocke* [2008] and *Liu et al.* [2009]. An equivalent way is to estimate the global electron content (GEC) of the ionosphere [*Afraimovich et al.*, 2008; *Astafyeva et al.*, 2008]. Here we symbolize the global average TEC as $\overline{\text{TEC}}$ for short. $\overline{\text{TEC}}$ can be understood as an imaginary ionosphere, in which TEC is distributed uniformly over the globe and, as a whole, has the same electron content as the actual ionosphere. The $\overline{\text{TEC}}$ is in units of TECu, where 1 TECu = 10^{16} electrons/m^2. As indicated by *Liu et al.* [2009], *Afraimovich et al.* [2008], and *Astafyeva et al.* [2008], either $\overline{\text{TEC}}$ or GEC excellently track the solar cycle variation and solar rotation modulations; thus it can be used as a practical ionospheric index. In other words, $\overline{\text{TEC}}$ should represent the global nature of the ionosphere. Therefore, $\overline{\text{TEC}}$ is an ideal parameter particularly for exploring the nature of the ionosphere under unusual solar activities.

2.3. Solar EUV and $F_{10.7}$

[10] Since 1996, solar full-disk EUV fluxes at two wavelength bands (26–34 nm and 0.1–50 nm) were continuously monitored by the Solar EUV Monitor (SEM) spectrometer aboard on the Solar Heliospheric Observatory (SOHO) satellite [*Judge et al.*, 1998], which accumulated the longest solar EUV records. The daily values of SEM/SOHO EUV fluxes at 1 AU are available at the Website (http://www.usc.edu/dept/space_science/). As statistically validated by *Liu et al.* [2006], there is a high correlation between the two wavelength bands of SOHO/SEM EUV fluxes. Thus, we just took the daily average values of the 26–34 nm band fluxes to scale the solar EUV intensity from January 1996 to October 2011.

[11] More importantly, although $F_{10.7}$ is popularly used as a standard solar proxy, a nonlinear relationship is found to exist in $F_{10.7}$ versus solar EUV fluxes [e.g., *Balan et al.*, 1994; *Richards et al.*, 1994; *Liu et al.*, 2006]. In contrast, a new parameter $F_{10.7P}$ introduced by *Hinteregger et al.* [1981] and *Richards et al.* [1994] becomes a better solar proxy to linearly describe the intensity of solar EUV fluxes fairly well in statistical sense, which was confirmed by *Liu et al.* [2006]. Here $F_{10.7P} = (F_{10.7} + F_{10.7A})/2$, and $F_{10.7A}$ is the 81 day centered mean of daily $F_{10.7}$. Therefore, we adopt $F_{10.7P}$ to measure the solar EUV intensity during the period when f_oF_2 data spanned, owing to lack of continuous observations of solar EUV spectrum.

[12] Daily values of $F_{10.7P}$ were deduced from the daily $F_{10.7}$ adjusted at 1 AU, which were provided at the SPIDR web site. A moving 1 year average procedure is applied to obtain the average values of $F_{10.7P}$ and the SOHO/SEM

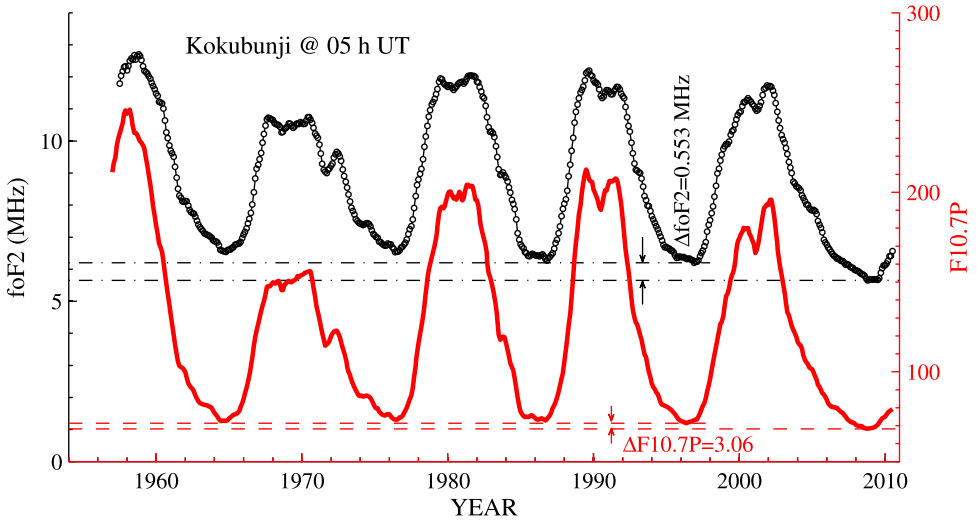

Figure 1. Moving 1 year mean of f_oF_2 at Kokubunji (35.7°N, 139.5°E) at 0500 UT and $F_{10.7P}$ over recent solar cycles. $F_{10.7P} = (F_{10.7} + F_{10.7A})/2$ in solar flux units (1 sfu = 10^{-22} W m^{-2} Hz^{-1}). Here $F_{10.7A}$ is the 81 day centered mean of $F_{10.7}$. The minimum value of f_oF_2 during solar minimum of cycle 23/24 is at least 0.553 MHz lower than those of the preceding cycles, and that of $F_{10.7P}$ in cycle 23/24 is 3.06 sfu lower than those in the preceding cycles.

EUV fluxes. Thus, we adopted both $F_{10.7P}$ and the SOHO/SEM EUV fluxes to characterize the intensity of solar EUV variability.

3. Results and Discussion

3.1. The f_oF_2 at Selected Stations

[13] Kokubunji (35.7°N, 139.5°E), a Japanese station, belongs to one of the stations having the longest continuous ionosonde measurements; so long data records from such a station are ideal for exploring this issue. Figure 1 plots the moving 1 year average of f_oF_2 since 1957 over Kokubunji at 0500 universal time (UT), or around 1400 local time (LT). The superposed solid line shows $F_{10.7P}$ with scales on the right. As shown in Figure 1, the Kokubunji f_oF_2 over four and a half solar cycles presents significant solar cycle variations, which has been investigated in many works [e.g., *Liu et al.*, 2006; *Chen et al.*, 2008; *Chen and Liu*, 2010]. The horizontal lines indicate that both f_oF_2 around 1400 LT and $F_{10.7P}$ went to the historical lowest in 2009. The differences of the minima of f_oF_2 around 1400 LT and $F_{10.7P}$ between solar cycles are 0.55 MHz and 3.06 solar flux units (sfu), respectively (1 sfu = 10^{-22} W m^{-2} Hz^{-1}). It should be pointed out that the similarities and differences of solar EUV and $F_{10.7}$ during 1996–2010 and f_oF_2 at Kokubunji, Okinawa (26.3°N, 127.8°E), and Wakkanai (45.4°N, 141.7°E) in different solar cycles have been discussed in detail by *Chen et al.* [2011].

[14] Figure 2 (left) depicts the local time dependence of Δf_oF_2, the differences of f_oF_2 minima at the solar minima

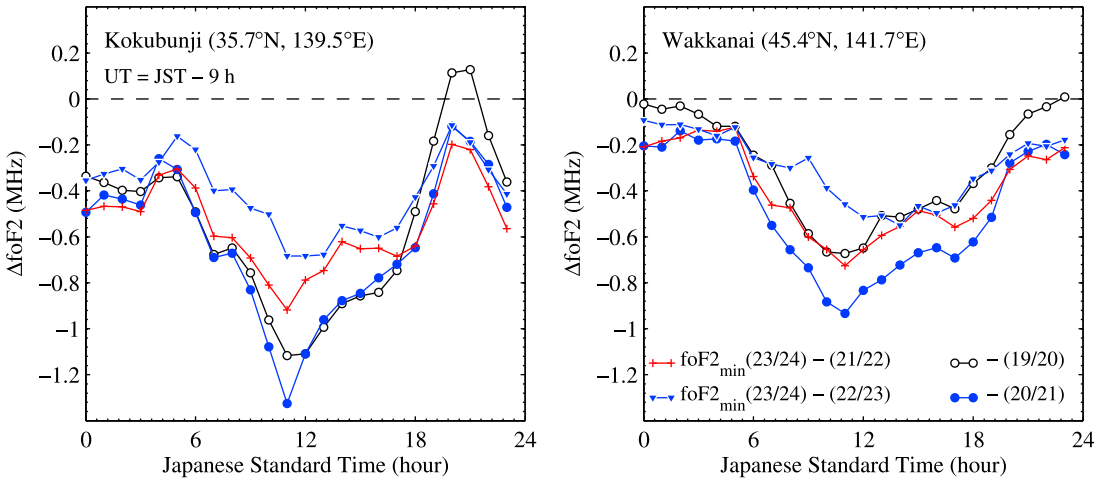

Figure 2. Local time dependence of the differences of minimum f_oF_2 between cycle 23/24 and the preceding cycles at Kokubunji (35.7°N, 139.5°E) and Wakkanai (45.4°N, 141.7°E).

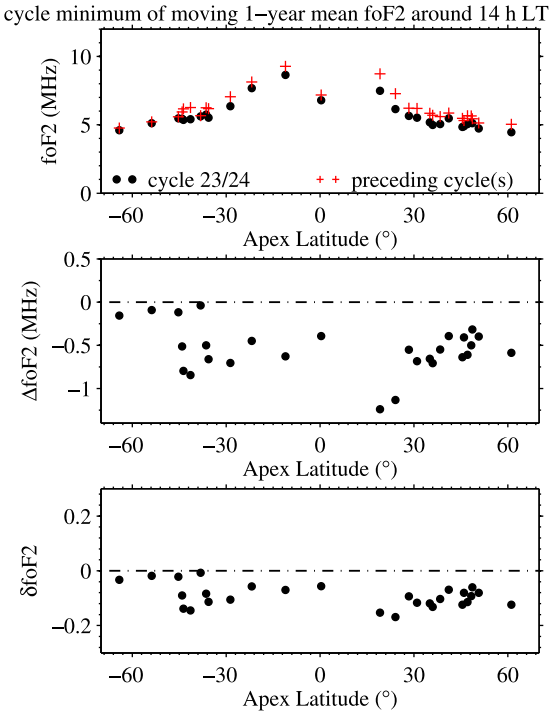

Figure 3. (top) The latitudinal profile of the minima of moving 1 year mean f_oF_2 around 1400 local time during cycle 23/24 and the preceding cycles. Corresponding (middle) absolute (Δf_oF_2) and (bottom) relative (δf_oF_2) differences.

between cycle 23/24 and the previous cycles (19/20, 20/21, 21/22, and 22/23) at Kokubunji. Figure 2 (right) gives the results of Δf_oF_2 at Wakkanai. Note that the horizontal axis indicates the Japanese standard time (JST, JST = UT + 9 h). The difference of local time at the two stations and JST is 0.3 h and 0.44 h, respectively.

[15] As shown in Figure 2, negative values appear in Δf_oF_2. There is a strong LT dependence in Δf_oF_2, larger during the daytime than at night. Moreover, the general local time pattern of Δf_oF_2 is somewhat similar over most stations. However, the values of Δf_oF_2 and its LT patterns at Kokubunji, Wakkanai and at other stations are not completely similar, which implies there is possibly of location difference. The spread in Δf_oF_2 reflects the fluctuations of f_oF_2 minima at the solar minima. As the reviewer commented, it also reflects the depth of the past solar minima relative to 23/24.

3.2. Global Pattern of Cycle Differences in f_oF_2, $h'F$, and f_oE Minima

[16] Due to the limitation of available stations, we ignore the possible longitudinal effect. To examine the global pattern of the features of ionosonde parameters, we organized the ionosonde stations listed in Table 1, according to the Apex latitude [*Richmond*, 1995]. Figure 3 (top) shows the latitudinal profile of the minima of moving 1 year mean f_oF_2 around 1400 local time during cycle 23/24 (dot points) and the preceding cycles (symbol "+"). For a station, if there are mean records available more than one solar minimum before 1998, we choose the minimum among these f_oF_2 minima. The corresponding absolute (Δf_oF_2) and relative (δf_oF_2) differences over these stations are presented in Figure 3 (middle and bottom).

[17] The cycle minimum values of f_oF_2 around 1400 LT as a function of Apex latitude indicate the existence of equatorial anomaly under solar minima. Meanwhile, the f_oF_2 minima in cycle 23/24 are prevailing lower than those in the preceding cycles. Thus, negative Δf_oF_2 prevails in Figure 3 (middle), and their values vary from −0.5 MHz to more than −1.2 MHz, except smaller differences at four stations. δf_oF_2 in Figure 3 (bottom) displays that the cycle differences in f_oF_2 minima reach to about 10%~18% at most stations.

[18] Due to lack of enough long records of the peak height of the F layer, we resorted to $h'F$ instead, to infer the altitude changes in the F layer. Figure 4 shows the results of $h'F$, in the same style of Figure 3. As was illustrated in Figure 4, the base of the F layer over most stations (14 out of 21) at solar minimum of cycle 23/24 is obviously lower than any time in the preceding cycles. However, an opposite change in $h'F$ appears at one northern hemisphere station, and no significant cycle differences in $h'F$ occur at other six stations. Overall, the decline of 10~20 km in the base altitude of the F layer is a dominant feature over the available stations. If $h'F$ may be taken as an indicator of changes in the F layer height, one would expect a reduction in the height of ionosphere, in good agreement with the conclusion of *Heelis et al.* [2009], in which they found the contraction of the ionosphere, according to the O^+/H^+ transition height being significantly smaller than was expected.

[19] Similar to Figures 3 and 4, Figure 5 plots the results of f_oE at 1400 LT. The minima of the moving 1 year average

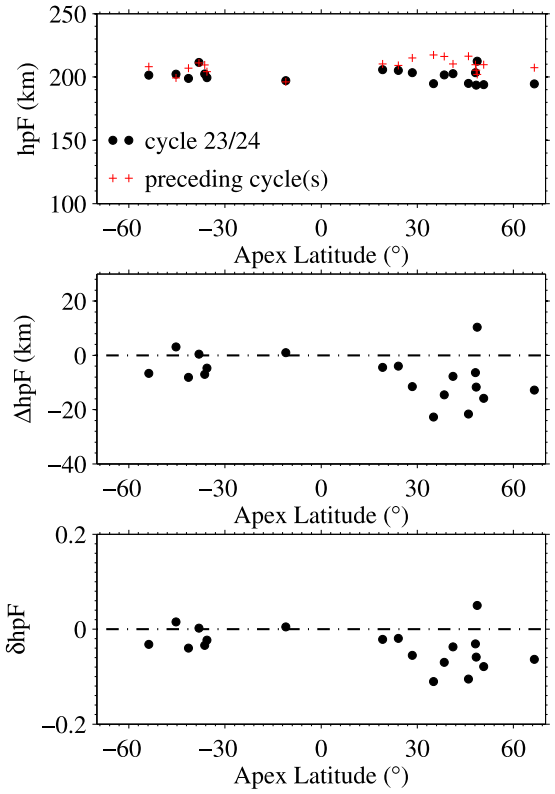

Figure 4. Similar to Figure 3 but for virtual height of F layer $h'F$.

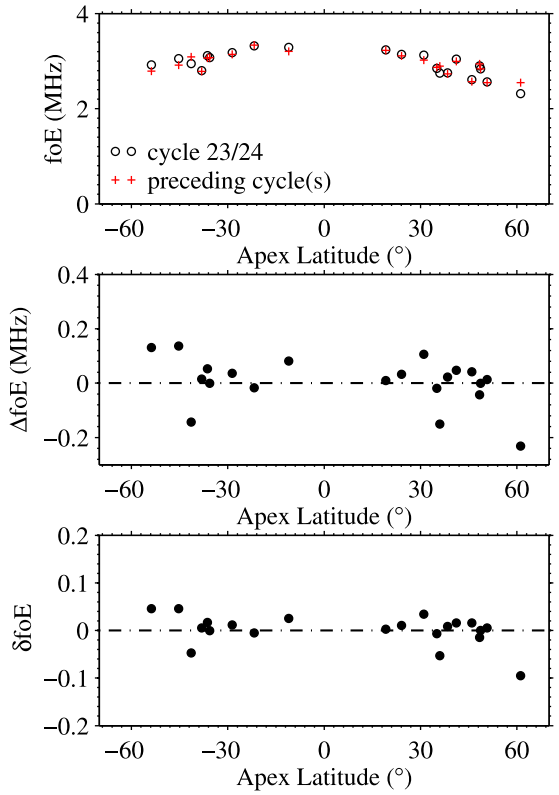

Figure 5. Similar to Figure 3 but for critical frequency of E layer f_oE.

f_oE at solar minima tend to be higher at lower latitudes, indicating the strong solar control on the E layer. The minima of f_oE over three stations decrease in cycle 23/24, compared to the preceding cycles, and smaller or no obvious variations in f_oE present at eight stations. It is worth noting that, whereas f_oE at remaining several stations shows an opposite change.

[20] The increase feature in Δf_oE around 1400 LT is compelling and quite interesting. It is well known that the E layer is strongly sensitive to changes in solar EUV; thus reduction in solar EUV is expected to a decrease in f_oE, which is opposite to the observed increase in f_oE over several stations. Note that, of course, this f_oE feature requires further confirmation from other sources, especially independent data sources. As we know, the accuracy of f_oE closely depends on the sensitivity of instrument. The normal E layer trace is often absent in some ionograms and under absorption cases. Moreover, the scaling of the normal E layer trace depends on the experience of ionogram interpretation, and the normal E layer trace is easily and possibly influenced by the Es traces. Taken together, the ionogram scaling may introduce a large uncertainty in the f_oE accuracy at some stations.

3.3. Global Average TEC Pattern

[21] Figure 6 shows the time series of daily values of SOHO/SEM EUV in 26–34 nm wavelength ranges since 1996 and the global average TEC ($\overline{\text{TEC}}$) during the years of 1998–2008. The thick lines denote the corresponding values moving averaged with a 1 year window.

[22] Initial analyses of $\overline{\text{TEC}}$ have been given by *Hocke* [2008] and *Liu et al.* [2009]. As illustrated in Figure 6, the daily values of $\overline{\text{TEC}}$ present variations with different time scales. Note that the variations of the moving average $\overline{\text{TEC}}$ denoted by thick lines follow those of EUV. With increasing (decreasing) solar activity, $\overline{\text{TEC}}$ tends to increase (decrease). A consistent pattern can also be detected is that, both $\overline{\text{TEC}}$ and solar EUV have two peaks in 2000 and 2002, respectively, and a trough in 2001. It provides evidence of the strong forcing of solar irradiance to the ionosphere. The horizontal lines show that, similar to $F_{10.7P}$ in Figure 1, the intensity of solar EUV is also lower in 2009 than in 1996 by 2.066×10^9 photons·cm^{-2}·s^{-1}. Unfortunately, the JPL GIMs are restricted to the period after the solar minimum of cycle 22/23; so no cycle difference of $\overline{\text{TEC}}$ minima can be offered here.

[23] The wavelet amplitude spectrum of GEC has been conducted by *Afraimovich et al.* [2008]. The technique of applying a moving average greatly suppresses the shorter-term variations, including seasonal and solar rotation effects and other shorter components (see *Liu et al.* [2009] for details).

3.4. An Unusual Ionosphere at Solar Minimum of Cycle 23/24?

[24] Figure 7 (top) shows a scatterplot of Kokubunji f_oF_2 versus $F_{10.7P}$ presented in Figure 1, and Figure 7 (bottom) plots $\overline{\text{TEC}}$ and SOHO/SEM EUV shown in Figure 6. Numbers 1996–2010 mark the points at the beginning of years in the recent solar cycle, respectively. A quadratic fitting is applied to the data prior to 2007 for estimating the statistical relationship as *Liu et al.* [2006, 2009] and *Liu and Chen* [2009] have done. A dotted line in each panel shows the fitted result.

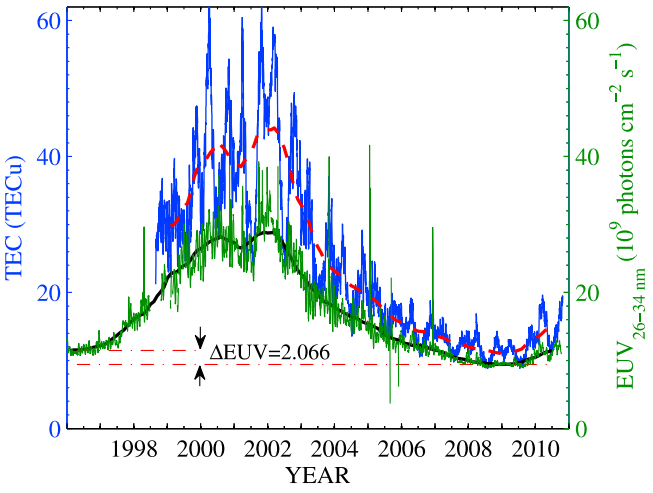

Figure 6. The daily SOHO/SEM solar full-disk EUV fluxes (in units of 10^9 photons cm^{-2} s^{-1}) at 26–34 nm wavelength band at 1 AU from 1996 to 2010 and the global average TEC (in units of 10^{16} electrons/m^2, denoted by TECu) of GPS-derived JPL global ionospheric maps (GIM) from 1998 to 2010, respectively. The superimposed lines denote the moving 1 year mean series. The EUV minimum in solar minimum of cycle 23/24 is 2.066×10^9 photons cm^{-2} s^{-1} lower than that of the preceding cycle.

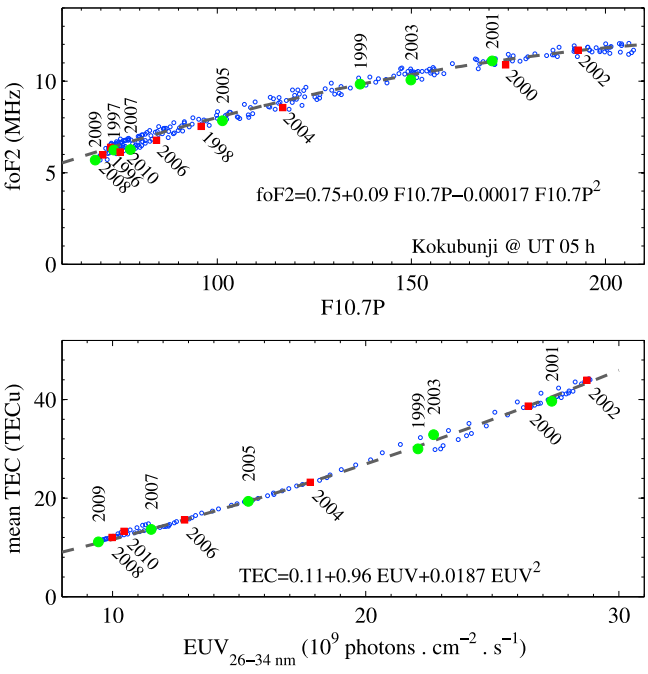

Figure 7. (top) Moving 1 year mean f_oF_2 versus $F_{10.7P}$ over the period from 1957 to 2010. $F_{10.7P} = (F_{10.7} + F_{10.7A})/2$ in solar flux units (1 sfu = 10^{-22} W m^{-2} Hz^{-1}). Here $F_{10.7A}$ is the 81 day centered mean of $F_{10.7}$. (bottom) The dependence of moving 1 year mean of global average JPL GPS TEC (in TECu; 1 TECu = 10^{16} electrons/m^2) on solar EUV flux at 26–34 nm wavelengths (in units of 10^9 photons cm^{-2} s^{-1}). SOHO/SEM recorded the daily average solar full-disk EUV flux in 26–34 and 0.1–50 nm wavelength intervals at 1 AU since 1995. The dotted curve and equation in each panel denotes a quadratic fitting of the data.

[25] The equation for Kokubunji f_oF_2 at 0500 UT is

$$f_oF_2 = 0.75 + 0.09\,F_{10.7P} - 0.00017F_{10.7P}^2, \quad (1)$$

and that for $\overline{\text{TEC}}$ is

$$\overline{\text{TEC}} = 0.11 + 0.96\ \text{EUV} + 0.0187\ \text{EUV}^2. \quad (2)$$

Equation (1) shows an apparent saturation feature in f_oF_2 over Kokubunji, and equation (2) reveals an amplification of $\overline{\text{TEC}}$ versus EUV; which are consistent with our previous analyses [*Liu et al.*, 2006, 2009; *Liu and Chen*, 2009].

[26] The fitting analyses support the conclusion of *Liu and Chen* [2009] fairly well; that is, a quadratic fitting can reasonably capture the statistical relation of f_oF_2 ($\overline{\text{TEC}}$) with $F_{10.7P}$ (EUV). Although only the data prior to 2007 were included for the fitting analysis, we can see from Figure 7 that equations (1) and (2) show their excellent predictability in predicting the values of f_oF_2 and $\overline{\text{TEC}}$ afterward.

[27] We would like to further use the fitting results as a baseline to discuss a topic: whether the ionosphere at solar minimum of cycle 23/24 is anomalous or predictable? The predicted f_oF_2 in 2009 at 0500 UT over Kokubunji is 5.99 MHz and the observed one is 5.68 MHz. The prediction uncertainty of f_oF_2 with this method is about 0.5 MHz [see *Liu et al.*, 2004]. Thus the small f_oF_2 offsets of the predicted values from the observed points are within the data scatters. In contrast, the $\overline{\text{TEC}}$ in 2007–2009 is predicted fairly well. According to the excellent predictions of equations (1) and (2) for f_oF_2 and $\overline{\text{TEC}}$ in 2007–2010, one important point can be implied is that the $\overline{\text{TEC}}$ under such extremely low solar conditions is explained by the reduction of solar EUV, and the decrease in f_oF_2 may be partly explained (about 0.3 MHz out of 0.55 MHz in Δf_oF_2). Thus, the ionosphere in 2007–2009 is unusual, but generally can be explained by the reduction in solar EUV. In other words, the main contributor to the record low of f_oF_2 and low $\overline{\text{TEC}}$ in 2007–2009 is the extremely low solar EUV during that period, whereas the gentle prediction deviations of f_oF_2 from observations do not reject the possible contributions from other sources.

4. Summary

[28] The above analysis provides evidence that a quadratic fitting can perfectly capture the statistical relation of f_oF_2 ($\overline{\text{TEC}}$) with $F_{10.7P}$ (EUV). It shows the tendency of f_oF_2 and $\overline{\text{TEC}}$ during such extremely low solar conditions may be predicted and explainable. More importantly, our results have outlined that the ionosphere in 2007–2009 was lower than typical solar minimum conditions, showing reductions in f_oF_2, $h'F$, and $\overline{\text{TEC}}$, which may be primarily contributed from the record low solar EUV during that period.

[29] The main unusual features of the solar activity during solar minimum in solar cycle 23/24 have been summarized by *Russell et al.* [2010]. The general unusual behaviors of the ionosphere under such extremely low solar activities are consistent with the pioneer simulations made by *Smithtro and Sojka* [2005]. The overall features of the F layer and $\overline{\text{TEC}}$ are also in good agreement with the unusual phenomena in the derived thermospheric density [*Solomon et al.*, 2010; *Emmert et al.*, 2010] and the upper transition height of O^+/H^+ [*Heelis et al.*, 2009]. Due to the limitation of stations available, unfortunately we cannot provide the longitude pattern in the ionosphere under such unusual solar conditions.

[30] Accompanying with the decline in solar EUV, f_oE is expected to decrease, according to the highly solar sensitivity of the E layer. Contrary to our expectation, however, a compelling feature is the increase of f_oE over some stations, which offers huge challenge for future researches to search for the real physical sources responsible for the different behavior of f_oE reported here.

[31] Additionally, the influence of increasing atmospheric concentrations of greenhouse gases to the upper atmosphere has become a popular topic. Over the past decades, although the Earth's surface temperature has increased, the lower and middle mesosphere has become cooler. Past studies revealed a slightly increasing in f_oE [*Laštovička and Bremer*, 2004; *Laštovička et al.*, 2006]. Therefore, if the increase in Δf_oE in 2007–2009 is a true feature, further investigations are required to assess the extent of the contribution from the positive trend in the secular changes in f_oE.

[32] **Acknowledgments.** Ionosonde data are provided from National Institute of Information and Communications Technology, Institute of Solar-Terrestrial Physics of Russia, and SPIDR. The JPL GIMs are produced and distributed by JPL. The $F_{10.7}$ index is also downloaded

from the SPIDR Web site. The SEM/SOHO EUV data are downloaded from the Web site http://www.usc.edu/dept/space_science/. We acknowledge the CELIAS/SEM experiment on the Solar Heliospheric Observatory (SOHO) spacecraft (SOHO is a joint European Space Agency and NASA mission). This research was supported by National Natural Science Foundation of China (40725014, 41074112), special fund for meteorology R&D (GYHY201106011), and the Specialized Research Fund for State Key Laboratories.

[33] Robert Lysak thanks Tamara Gulyaeva and another reviewer for their assistance in evaluating this paper.

References

Afraimovich, E. L., E. I. Astafyeva, A. V. Oinats, Y. V. Yasukevich, and I. V. Zhivetiev (2008), Global electron content: A new conception to track solar activity, *Ann. Geophys.*, *26*, 335–344, doi:10.5194/angeo-26-335-2008.

Astafyeva, E. I., E. L. Afraimovich, A. V. Oinats, Y. V. Yasukevich, and I. V. Zhivetiev (2008), Dynamics of global electron content in 1998–2005 derived from global GPS data and IRI modeling, *Adv. Space Res.*, *42*, 763–769, doi:10.1016/j.asr.2007.11.007.

Balan, N., G. J. Bailey, B. Jenkins, P. B. Rao, and R. J. Moffett (1994), Variations of ionospheric ionization and related solar fluxes during an intense solar cycle, *J. Geophys. Res.*, *99*, 2243–2253, doi:10.1029/93JA02099.

Bilitza, D., and B. W. Reinisch (2008), International Reference Ionosphere 2007: Improvements and new parameters, *Adv. Space Res.*, *42*, 599–609, doi:10.1016/j.asr.2007.07.048.

Chen, Y., and L. Liu (2010), Further study on the solar activity variation of daytime N_mF_2, *J. Geophys. Res.*, *115*, A12337, doi:10.1029/2010JA015847.

Chen, Y., L. Liu, and H. Le (2008), Solar activity variations of nighttime ionospheric peak electron density, *J. Geophys. Res.*, *113*, A11306, doi:10.1029/2008JA013114.

Chen, Y., L. Liu, and W. Wan (2011), Does the $F_{10.7}$ index correctly describe solar EUV flux during the deep solar minimum of 2007–2009?, *J. Geophys. Res.*, *116*, A04304, doi:10.1029/2010JA016301.

Emmert, J. T., J. L. Lean, and J. M. Picone (2010), Record-low thermospheric density during the 2008 solar minimum, *Geophys. Res. Lett.*, *37*, L12102, doi:10.1029/2010GL043671.

Gibson, S. E., J. U. Kozyra, G. de Toma, B. A. Emery, T. Onsager, and B. J. Thompson (2009), If the Sun is so quiet, why is the Earth ringing? A comparison of two solar minimum intervals, *J. Geophys. Res.*, *114*, A09105, doi:10.1029/2009JA014342.

Gorney, D. J. (1990), Solar cycle effects on the near-Earth space environment, *Rev. Geophys.*, *28*, 315–336, doi:10.1029/RG028i003p00315.

Heelis, R. A., et al. (2009), Behavior of the O+/H+ transition height during the extreme solar minimum of 2008, *Geophys. Res. Lett.*, *36*, L00C03, doi:10.1029/2009GL038652.

Hinteregger, H. E., K. Fukui, and B. R. Gilson (1981), Observational, reference and model data on solar EUV, from measurements on AE-E, *Geophys. Res. Lett.*, *8*, 1147–1150, doi:10.1029/GL008i011p01147.

Hocke, K. (2008), Oscillations of global mean TEC, *J. Geophys. Res.*, *113*, A04302, doi:10.1029/2007JA012798.

Iijima, B. A., I. L. Harris, C. M. Ho, U. J. Lindqwister, A. J. Mannucci, X. Pi, M. J. Reyes, L. C. Sparks, and B. D. Wilson (1999), Automated daily process for global ionospheric total electron content maps and satellite ocean altimeter ionospheric calibration based on global positioning system data, *J. Atmos. Sol. Terr. Phys.*, *61*, 1205–1218, doi:10.1016/S1364-6826(99)00067-X.

Judge, D., et al. (1998), First solar EUV irradiances obtained from SOHO by the SEM, *Sol. Phys.*, *177*, 161–173, doi:10.1023/A:1004929011427.

Kutiev, I., and P. Marinov (2007), Topside sounder model of scale height and transition height characteristics of the ionosphere, *Adv. Space Res.*, *39*, 759–766, doi:10.1016/j.asr.2006.06.013.

Laštovička, J., and J. Bremer (2004), An overview of long-term trends in the lower ionosphere below 120 km, *Surv. Geophys.*, *25*, 69–99, doi:10.1023/B:GEOP.0000015388.75164.e2.

Laštovička, J., R. A. Akmaev, G. Beig, J. Bremer, and J. T. Emmert (2006), Global change in the upper atmosphere, *Science*, *314*, 1253–1254, doi:10.1126/science.1135134.

Liu, L., and Y. Chen (2009), Statistical analysis on the solar activity variations of the TEC derived at JPL from global GPS observations, *J. Geophys. Res.*, *114*, A10311, doi:10.1029/2009JA014533.

Liu, L., W. Wan, and B. Ning (2004), Statistical modeling of ionospheric f_oF_2 over Wuhan, *Radio Sci.*, *39*, RS2013, doi:10.1029/2003RS003005.

Liu, L., W. Wan, B. Ning, O. M. Pirog, and V. I. Kurkin (2006), Solar activity variations of the ionospheric peak electron density, *J. Geophys. Res.*, *111*, A08304, doi:10.1029/2006JA011598.

Liu, L., W. Wan, B. Ning, and M.-L. Zhang (2009), Climatology of the mean TEC derived from GPS global ionospheric maps, *J. Geophys. Res.*, *114*, A06308, doi:10.1029/2009JA014244.

Liu, L., M. He, X. Yue, B. Ning, and W. Wan (2010), The ionosphere around equinoxes during low solar activity, *J. Geophys. Res.*, *115*, A09307, doi:10.1029/2010JA015318.

Liu, L., W. Wan, Y. Chen, and H. Le (2011), Solar activity effects of the ionosphere: A brief review, *Chin. Sci. Bull.*, *56*(12), 1202–1211, doi:10.1007/s11434-010-4226-9.

Lühr, H., and C. Xiong (2010), The IRI-2007 model overestimates electron density during the 23/24 solar minimum, *Geophys. Res. Lett.*, *37*, L23101, doi:10.1029/2010GL045430.

Mannucci, A. J., B. D. Wilson, D. N. Yuan, C. M. Ho, U. J. Lindqwister, and T. F. Runge (1998), A global mapping technique for GPS derived ionospheric total electron content measurements, *Radio Sci.*, *33*, 565–582, doi:10.1029/97RS02707.

Richards, P. G., J. A. Fennelly, and D. G. Torr (1994), EUVAC: A solar EUV flux model for aeronomic calculations, *J. Geophys. Res.*, *99*, 8981–8992, doi:10.1029/94JA00518.

Richmond, A. D. (1995), Ionospheric electrodynamics using magnetic apex coordinates, *J. Geomagn. Geoelectr.*, *47*, 191–212.

Russell, C. T., J. G. Luhmann, and L. K. Jian (2010), How unprecedented a solar minimum?, *Rev. Geophys.*, *48*, RG2004, doi:10.1029/2009RG000316.

Smithtro, C. G., and J. J. Sojka (2005), Behavior of the ionosphere and thermosphere subject to extreme solar cycle conditions, *J. Geophys. Res.*, *110*, A08306, doi:10.1029/2004JA010782.

Solomon, S. C., T. N. Woods, L. V. Didkovsky, J. T. Emmert, and L. Qian (2010), Anomalously low solar extreme-ultraviolet irradiance and thermospheric density during solar minimum, *Geophys. Res. Lett.*, *37*, L16103, doi:10.1029/2010GL044468.

Y. Chen, H. Le, and L. Liu, Beijing National Observatory of Space Environment, Institute of Geology and Geophysics, Chinese Academy of Sciences, 19 Beitucheng Western Rd., Beijing 100029, China. (liul@mail.iggcas.ac.cn)

V. I. Kurkin and N. M. Polekh, Institute of Solar-Terrestrial Physics, Russian Academy of Sciences, PO Box 291, Lermontov St. 126a, Irkutsk 664033, Russia.

C.-C. Lee, General Education Center, Ching-Yun University, Jhungli 320, Taiwan. (cclee@cyu.edu.tw)